Evaluation of an adjoint-based liner impedance eduction technique

J. Primus, E. Piot and F. Simon

ONERA - The French Aerospace Lab, 2 av Edouard Belin, F-31055 Toulouse, France
julien.primus@onera.fr

This paper describes a new method for acoustic liner impedance eduction. The eduction process aims at finding the liner impedance which minimizes the error between numerical simulations and a set of measured data. The method relies on the resolution of the two-dimensional Linearized Euler Equations in the frequency domain, spatially discretized by a Discontinuous Galerkin scheme. The minimization of the objective function is achieved by the resolution, at each iteration, of the direct and adjoint equations. This leads to an analytical expression of the objective function derivatives. The process is benchmarked on pressure measurements found in the literature, in a no-flow configuration. Results compare very favorably to the reference curves, except at the anti-resonance frequency of the material where a small discrepancy occurs. A numerical investigation is also made to show the possibility to educe liner impedance from acoustic velocity measurements.

1 Introduction

To reduce the noise generated by the turbofans, aircraft manufacturers usually mount acoustic treatments in the nacelle. These liners are typically made of honeycomb cells topped by a perforated sheet, working on the principle of Helmholtz resonators. Optimization of the resulting passive noise reduction requires an accurate knowledge of the acoustic liner properties in the conditions of use, which include the presence of a grazing flow. These properties are represented by the acoustic impedance, an homogenized quantity defined locally as the ratio between the acoustic pressure at the surface of the material over the normal acoustic velocity. Various methods exist for the measurement of liner acoustic impedance with grazing flow. Dean [1] introduced an *in-situ* technique relying on two microphone measurements respectively at the rear wall of the liner cavity and at the surface of the perforated sheet, associated to a propagation model inside the cavity. At ONERA, the acoustic impedance is deduced from Laser Doppler Velocimetry (LDV) measurements above the liner. To access the acoustic pressure at the surface of the perforated sheet, these velocity measurements are combined to either a Galbrun propagation model [2] or to acoustic pressure measurements [13].

Over the past few years, the limitations of existing techniques motivated the development of inverse methods for liner impedance eduction. The principle is to use a numerical or analytical propagation model to find the liner impedance which, in the best possible way, reproduces acoustic measurements made in a duct test rig. To achieve this, an objective function representative of the distance between measured and simulated quantities is minimized. NASA has brought valuable contribution with a robust method based on acoustic pressure measurements on the rigid wall opposite the test liner [3] and a finite element model. Indirect processes based on a 3-zones duct model (upstream, above and downstream of the liner) with a mode matching approach are also used [4, 5]. However these methods can suffer from the lack of information nearby the lining sample.

A new eduction method is currently being developed at ONERA. It is planned to be based on velocity measurements acquired by LDV above the liner. The propagation model relies on the two-dimensional Linearized Euler Equations (LEE) in the frequency domain to account for a sheared flow profile in further developments. The gradient of the objective function is calculated thanks to the adjoint system of equations. This offers the advantage to provide an analytical expression for the derivatives, while the finite difference method generally used introduces approximation errors and has a computational cost which increases with the number of search parameters. Both direct and adjoint system are spatially discretized by a Discontinuous Galerkin (DG) scheme, which particularly suits the considered problem in the way to express the boundary conditions.

In section 2, the governing equations and the discretization scheme are presented. The principle of the impedance eduction process is then exposed in section 3. Benchmarking is done in section 4 with data available in the literature, before introducing the velocity-based eduction process and giving some concluding remarks.

2 Governing equations and numerical method

2.1 Propagation model

The propagation model relies on the two-dimensional LEE. A steady incompressible mean flow, with velocity U_0 along the streamwise coordinate x_1 and V_0 along the transversal coordinate x_2, is subject to an acoustic perturbation $\varphi = (u, v, p)^\intercal$. The duct configuration typically considered is shown on figure 1.

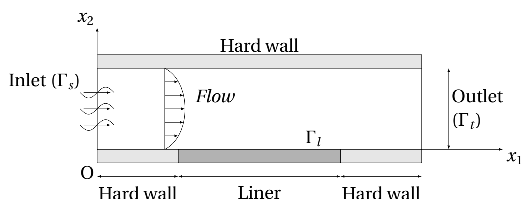

Figure 1: Generic geometry of the duct

The governing equations are written in a dimensionless matrix form, for an $e^{j\omega t}$ time dependence:

$$j\omega\varphi + \mathbf{A}^i\partial_i\varphi + \mathbf{B}\varphi = 0 \tag{1}$$

with

$$\mathbf{A}^1 = \begin{pmatrix} U_0 & 0 & 1 \\ 0 & U_0 & 0 \\ 1 & 0 & U_0 \end{pmatrix}, \mathbf{A}^2 = \begin{pmatrix} V_0 & 0 & 0 \\ 0 & V_0 & 1 \\ 0 & 1 & V_0 \end{pmatrix} \tag{2}$$

and

$$\mathbf{B} = \begin{pmatrix} \partial_1 U_0 & \partial_2 U_0 & 0 \\ \partial_1 V_0 & -\partial_1 U_0 & 0 \\ 0 & 0 & 0 \end{pmatrix} \tag{3}$$

The symbol ∂_i ($i \in [\![1, 2]\!]$) represents the spatial derivative with respect to the coordinate x_i. Velocities are nondimensionalized by c_0, pressures by $\rho_0 {c_0}^2$, lengths by the duct height H and time by H/c_0. The speed of sound c_0 and the density ρ_0 of the mean flow are considered uniform.

A Discontinuous Galerkin formulation is used to solve these equations numerically. The domain is partitioned into

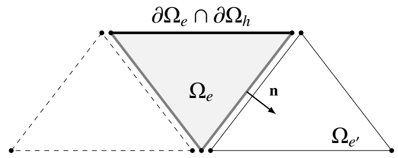

Figure 2: An element Ω_e adjacent to the computational boundary.

Lagrange $\mathbb{P}_1$ elements denoted Ω_e (see figure 2). The numerical solution vector over an element is written φ_h^e. A variational formulation is established over the element Ω_e for a test function ψ_h^e:

$$\int_{\Omega_e} \left(j\omega\varphi_h^e + \mathbf{A}^i\partial_i\varphi_h^e + \mathbf{B}\varphi_h^e \right) \cdot \psi_h^e \,\mathrm{d}\Omega_e + \sum_{k=1}^{3} \int_{\partial\Omega_{e,k}} \mathbf{F}(\varphi_h^{e-}, \varphi_h^{e+}, \mathbf{n}) \cdot \psi_h^{e-} \,\mathrm{d}\Gamma = 0 \quad (4)$$

where the superscript "$^-$" (resp. "$^+$") indicates the interior (resp. exterior) trace of the solution. It is the value of φ_h^e inside (resp. outside) the element Ω_e at an interface with other elements or with the domain boundary, depending on the edge k considered. $\mathbf{n} = n_i x_i$ is the outward unit normal to the boundary $\partial\Omega_e$. The function $\mathbf{F}(\varphi_h^{e-}, \varphi_h^{e+}, \mathbf{n})$ describes the connection to the neighbouring elements and the boundary conditions, and includes the choice of a numerical flux which will not be detailed here for the sake of brevity. Several cases are to be considered for the expression of $\mathbf{F}$.

- The edge is an internal edge. Incoming and outgoing waves are distinguished using the hyperbolic properties of the equations, which allows to build an upwind numerical flux. Then:

  $$\mathbf{F}(\varphi_h^{e-}, \varphi_h^{e+}, \mathbf{n}) = \mathbf{A}^i n_i^- \left(\varphi_h^{e+} - \varphi_h^{e-} \right) \quad (5)$$

  with $\mathbf{A}^i n_i^-$ the matrix corresponding to the negative eigenvalues of $\mathbf{A}^i n_i$.

- The source boundary condition is introduced through a vector φ_0 by writing:

  $$\mathbf{F}(\varphi_h^{e-}, \varphi_h^{e+}, \mathbf{n}) = \mathbf{A}^i n_i^- \left(\varphi_0 - \varphi_h^{e-} \right) \quad (6)$$

- Non-reflective boundary conditions are achieved by cancelling the incoming waves, leading to a characteristic boundary condition described by:

  $$\mathbf{F}(\varphi_h^{e-}, \varphi_h^{e+}, \mathbf{n}) = -\mathbf{A}^i n_i^- \varphi_h^{e-} \quad (7)$$

- The impedance boundary condition, which plays a key role in the present problematic, is written:

  $$\mathbf{F}(\varphi_h^{e-}, \varphi_h^{e+}, \mathbf{n}) = \mathbf{M}_\beta \varphi_h^{e-} \quad (8)$$

  where

  $$\mathbf{M}_\beta = \frac{1}{2} \begin{pmatrix} (\beta+1)\,\mathbf{n}\otimes\mathbf{n} & -(1-\beta)\mathbf{n} \\ -(1+\beta)\mathbf{n}^\intercal & (1-\beta) \end{pmatrix} \quad (9)$$

  $\beta = \frac{z-1}{z+1}$ is the reflection coefficient. The above impedance condition expresses the classical definition of the normalized specific impedance z:

  $$z = \frac{p}{v^i n_i} = \frac{p}{v_n} \quad (10)$$

The use of a β-formulation instead of a z-formulation avoids singularities to arise in the case of rigid walls. Note that contrary to most of similar methods, the Ingard-Myers [6] condition is not required as the process is intended to be used with no flow or with sheared flow profiles.

The final formulation is easily obtained by expressing φ_h^e and ψ_h^e as a linear combination of the basis functions and by summing over all the elements.

2.2 Adjoint system of equation

The eduction process requires the minimization of an objective function $\mathcal{J}$ describing the distance over an observation region between measured and calculated data. A general form of this objective function is:

$$\mathcal{J} = \int_\Omega \|\varphi_{calc} - \varphi_{meas}\|^2 \, I_{\Omega_{obs}}(\mathbf{x}) \quad (11)$$

where $I_{\Omega_{obs}}(\mathbf{x})$ is the indicator function of the observation region Ω_{obs} such as

$$I_{\Omega_{obs}}(\mathbf{x}) = \begin{cases} 1 & \text{if } \mathbf{x} \in \Omega_{obs} \\ 0 & \text{if } \mathbf{x} \notin \Omega_{obs} \end{cases} \quad (12)$$

At each iteration of the eduction process, the gradient of $\mathcal{J}$ is needed to find a new set of parameters which should lead to a smaller objective function. The gradient is often calculated by means of a finite difference method, but this leads to an approximate result and a calculation cost increasing with the number of parameters to be educed. Use of the adjoint equations allows on the other hand to obtain an analytical expression for the derivatives of $\mathcal{J}$.

If the liner impedance z_l is obviously a search parameter to be considered, a choice has to be made regarding which other quantities should be included in the eduction process as parameters. Eversman & Gallman [7] propose an eduction method where termination impedance and effective Mach number are parameters of the search process. The method presented here includes termination impedance z_t, as well as a calibration coefficient $C \in \mathbb{C}$ to adjust the amplitude and phase of the source to the measurements.

The adjoint system of equations may be determined by the method of Lagrange multipliers, considering the direct equations (1) and the associated boundary conditions as constraints. The adjoint state is defined as the Lagrange multiplier φ^* satisfying the following system, called "adjoint system":

$$\begin{cases} -j\omega\varphi^* - \partial_i \left(\mathbf{A}^{i\dagger} \varphi^* \right) + \mathbf{B}^\dagger \varphi^* = \partial_\varphi \mathcal{J} & \text{on } \Omega \\ \mathbf{M}_\beta^* \varphi^* = 0 & \text{on } \Gamma_l \\ \mathbf{A}^i n_i^+ \varphi^* = 0 & \text{on } \Gamma_t \cup \Gamma_s \end{cases} \quad (13)$$

The symbol $\dagger$ denotes the Hermitian conjugate. The adjoint impedance matrix is given by $\mathbf{M}_\beta^* = \mathbf{A}^i n_i + \mathbf{M}_\beta^\dagger$. Further details on the determination of the adjoint system can be found for example in [8] in the case of an optimal control problem.

The directional derivatives of the objective function can then be expressed as a function of the direct and adjoint states:

$$\frac{\partial \mathcal{J}(\varphi, z, C)}{\partial z_l} = -\langle \frac{\partial \mathbf{M}_\beta}{\partial \beta} \frac{\partial \beta}{\partial z_l} \varphi, \varphi^* \rangle_{\Gamma_l} \quad (14)$$

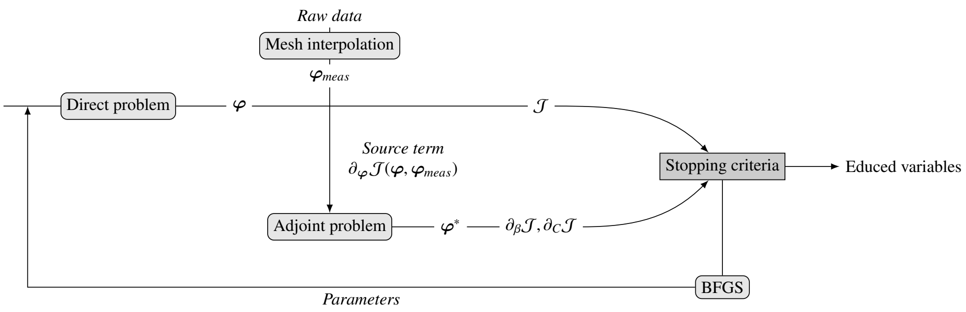

Figure 3: Diagram of the eduction process

and

$$\frac{\partial \mathcal{J}(\varphi, z, C)}{\partial C} = \langle \mathbf{A}^i n_i^- \varphi_0, \varphi^* \rangle_{\Gamma_s} \tag{15}$$

Equation (14) also holds for the termination Γ_t, described by an impedance z_t.

3 Impedance eduction process

At each iteration on the search parameters, the direct and adjoint equations are solved. As the derivative of $\mathcal{J}$ with respect to φ appears in the right-hand side of the adjoint equation (13), the direct system must be considered before the adjoint system. Once the adjoint equations are solved, at a computational cost comparable to the resolution of the direct equations, the gradient of $\mathcal{J}$ is calculated with equations (14) and (15). A new set of search parameters is then defined by a BFGS algorithm [9] to reduce $\mathcal{J}$ until one of the stopping criteria is met.

The global eduction loop is synthesized on figure 3. Note that an interpolation of the raw test data is necessary since generally the nodes of the numerical mesh do not match the location of experimental points.

4 Benchmark with pressure measurements

The propagation model presented above has already been validated on academic test-cases and compared with experimental results in a previous paper [10]. Benchmarking of the eduction process is realized here on data published by the NASA Langley Research Center [11]. In this reference paper, the authors educe the acoustic impedance thanks to a finite element model of the convected Helmholtz equation and acoustic pressure measurements at the rigid wall opposite the lining sample.

Using these acoustic pressure measurements, in the case without flow, our eduction process has been applied with the following objective function:

$$\mathcal{J}(\varphi, z, C) = \sum_{m=1}^{N} \| p_{calc}^m - p_{meas}^m \|^2 \tag{16}$$

where N=31 is the total number of microphones.

Two analyses have been conducted: the “NRp” case uses a non-reflective boundary condition (equivalent to $z_t = 1.00 + 0.00j$) at the termination plane, whereas in the “EIp” case the exit impedance is included as a search parameter. The configuration of the duct is represented on figure 4.

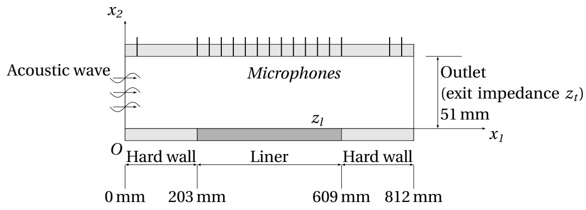

Figure 4: Geometry of the NASA Grazing Incidence Tube (GIT)

The comparison between exit and liner impedance values educed with the method presented here and the NASA values is presented on figures 5 and 6. The results compare very favorably to the reference. The only discrepancy occurs at 2 kHz which is the anti-resonance frequency of the studied liner, where attenuation is minimal. The difficulties experienced by eduction methods at anti-resonance have already been observed and are presently under consideration [12]. This can be illustrated by the fact that the objective function is not very sensitive to changes in the impedance at this frequency, as indicated by the flat valley around the minimum on figure 7. On this figure, the objective function has been made dimensionless so that it can be interpreted as an error on the target value:

$$\mathcal{J}_{red} = \frac{\sum_{m=1}^{N} \| p_{calc}^m - p_{meas}^m \|^2}{\sum_{m=1}^{N} \| p_{meas}^m \|^2} \tag{17}$$

It appears that a 0.5 % error only is made on the objective function with a resistance varying from 2.6 to 4.8 and a reactance varying from 0.8 to 3.0. Thus a quite large change in the impedance has only little effect on the acoustic field, as the liner tends to behave as a rigid wall.

Please note that the NASA educed value located on figure 7 is only shown for information. It appears less close to the minimum since it has been educed with a code different from the DG code used to draw the objective function. The same plot done with the NASA code would show the NASA educed value at the minimum.

5 Numerical investigation on a velocity-based objective function

In further developments, the eduction method is planned to be used with acoustic velocity measurements obtained by LDV. Before testing the process with real measurements, the feasability of impedance eduction relying on an objective

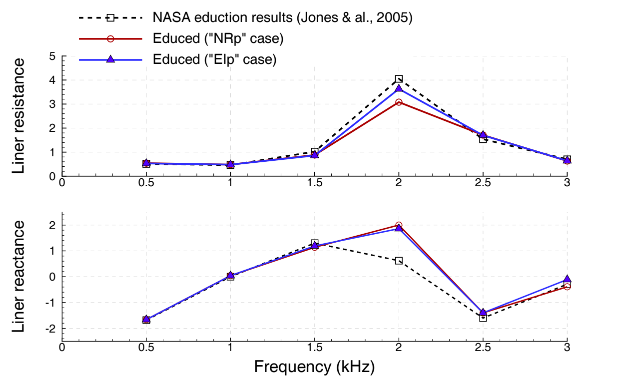

Figure 5: Liner impedance educed from upper wall pressure measurements on the NASA GIT

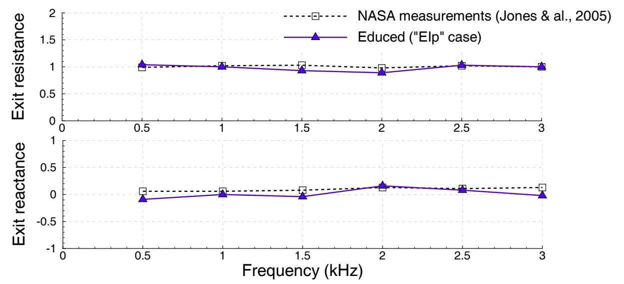

Figure 6: Exit impedance educed from upper wall pressure measurements on the NASA GIT for the "EIp" case.

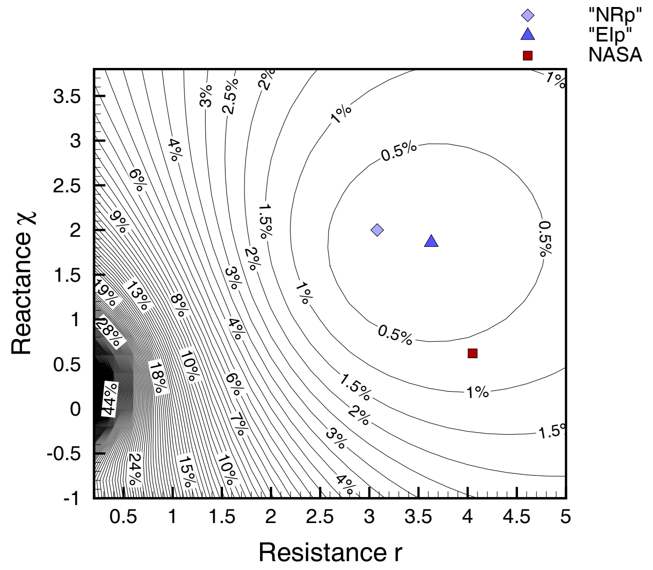

Figure 7: Objective function based on the acoustic pressure, represented at 2 kHz in the impedance plane (r, χ). The exit impedance and calibration coefficient are fixed to their educed values. Symbols locate the educed impedances.

function expressed in terms of acoustic velocity must be established.

A numerical experimentation has been made, in which the configuration is the same as in section 4. Propagation simulations are performed, with the NASA impedances as input of the DG code, providing acoustic velocity fields on the whole domain. These calculated fields will be considered here as the experimental results. The eduction process applied to these synthesized data should of course lead to the input impedance values. The observation region is chosen to match the typical area covered by LDV, and is represented on figure 8. It consists in a 20 mm-height rectangular area above the liner. It offers the advantage to be two-dimensional and to be very close to the liner, where the absorption effects are the most visible. This case will be denoted "EIv" case.

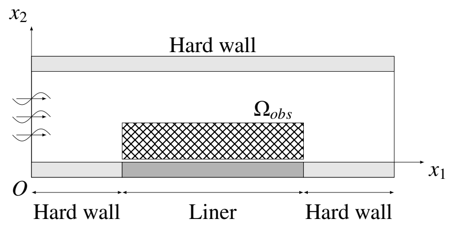

Figure 8: Observation region for the "EIv" case

The objective function in terms of velocity reads:

$$\mathcal{J}(\varphi, z, C) = \int_{\Omega} \|\mathbf{u}_{meas} - \mathbf{u}_{calc}\|^2 \, I_{\Omega_{obs}}(\mathbf{x}) \tag{18}$$

Eduction results are presented on figure 9 and figure 10 for the liner and exit impedance, respectively. As expected, the educed values perfectly match the input impedances, which confirms that eduction with a velocity-based objective function is possible. Of course the synthesized velocity does not suffer from measurement noise and a sensitivity study to added noise still has to be carried out.

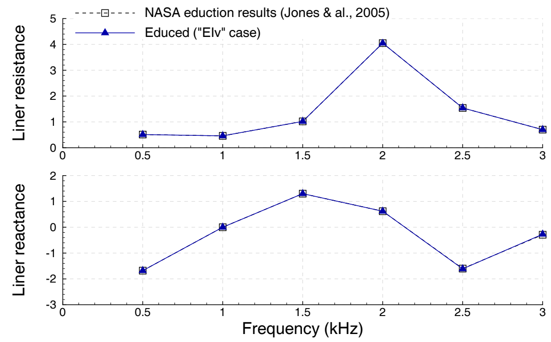

Figure 9: Liner impedance educed from simulated velocity ("EIv" case) on the NASA GIT.

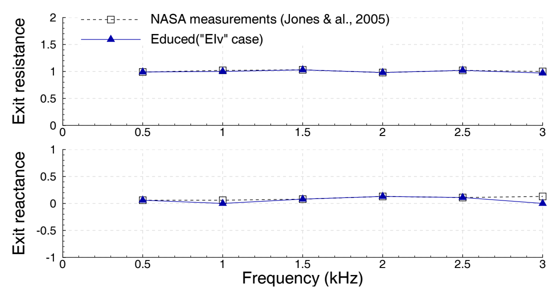

Figure 10: Exit impedance educed from simulated velocity ("EIv" case) on the NASA GIT.

6 Concluding remarks

A new method for liner impedance eduction has been presented, with the specificity of involving the adjoint system to calculate the objective function derivatives. This allows to obtain an analytical expression for the gradient, and to include easily a number of parameters other than the liner impedance, at a computational cost which remains unchanged.

The method has been tested and validated against NASA results available in the literature. Only few results are presented in this paper for the sake of brevity, but they show very good agreement with the reference plots. The possible use of an objective function expressed in terms of acoustic velocity has been checked. It will allow the development of an eduction process based on LDV measurements, which give access to information very close to the liner.

A number of studies are currently being carried out, including a sensitivity study of the impedance educed values to the measurement noise generated by the instrumental system and the signal processing. LDV measurements with and without flow on microperforated liners have been performed and are under consideration at the moment. Finally, it could be interesting to consider the optimal control problem associated to our configuration to obtain an adjoint field giving indication on the best possible observation region.

References

[1] P.D. Dean, "An *in situ* method of wall acoustic impedance measurement in flow duct", *Journal of Sound and Vibration* **34**(1), 97-130 (1974)

[2] M. Lavieille, F. Simon, F. Micheli, "Measurement of liner acoustic impedance in a shear layer of a subsonic flow by Laser Doppler Velocimetry ", *in: SAPEM* (2005)

[3] W.R. Watson, M.G. Jones, C.H. Gerhold, "Implementation and validation of an impedance eduction technique", *in: Proceedings of the 17th AIAA/CEAS Aeroacoustics Conference*, AIAA 2011-2867 (2011)

[4] T. Elnady, H. Bodén, "An inverse analytical method for extracting liner impedance from pressure measurements", *in: Proceedings of the 10th AIAA/CEAS Aeroacoustics Conference*, AIAA 2004-2836 (2004)

[5] Y. Aurégan, M. Leroux, V. Pagneux, "Measurement of liner impedance with flow by an inverse method", *in: Proceedings of the 10th AIAA/CEAS Aeroacoustics Conference*, AIAA 2004-2838 (2004)

[6] M.K. Myers, "On the acoustic boundary condition in the presence of flow", *Journal of Sound and Vibration* **71**(3), 429-434 (1980)

[7] W. Eversman, J.M. Gallman, "Impedance eduction with an extended search procedure", *AIAA Journal* **49**(9), 1960-1970 (2011)

[8] S. Walther, C. Airiau, A. Bottaro, "Optimal control of Tollmien-Schlichting waves in a developing boundary layer", *Physics of Fluids* **13**(7), 2087-2096 (2001)

[9] C. Zhu, R.H. Byrd, P. Lu, J. Nocedal, "L-BFGS-B: Algorithm 778: L-BFGS-B, FORTRAN routines for large scale bound constrained optimization", *ACM Transactions on Mathematical Software* **23**(4), 550-560 (1997)

[10] J. Primus, F. Simon, E. Piot, "Validation of a direct propagation model for liner impedance eduction", *in: Proceedings of the 17th AIAA/CEAS Aeroacoustics Conference*, AIAA 2004-2869 (2011)

[11] M.G. Jones, W.R. Watson, T.L. Parrott, "Benchmark data for evaluation of aeroacoustic propagation codes with grazing flow", *in: Proceedings of the 10th AIAA/CEAS Aeroacoustics Conference*, AIAA 2011-2853 (2005)

[12] M.G. Jones, W.R. Watson, "On the use of experimental methods to improve confidence in educed impedance", *in: Proceedings of the 17th AIAA/CEAS Aeroacoustics Conference*, AIAA 2011-2865 (2011)

[13] B. Nennig, M. Ben Tahar, J.M. Ville, E. Piot, F. Simon, M. Taktak, "A comparison between acoustic liner characterization methods and calculations", *in: Proceedings of the 16th International Congress on Sound and Vibration* (2009)